A Role of Remote Sensing Analysis for Archaeological Purposes in Arid Climate Regions

Supplementary Materials for https://doi.org/10.5194/egusphere-egu24-2892

Lev V. Eppelbaum[1,2], Olga Khabarova[1] and Michal Birkenfeld[3]

[1]Department of Geophysics, Tel Aviv University, Ramat Aviv, Tel Aviv, Israel (Email: levap@tauex.tau.ac.il)
[2]Azerbaijan State Oil and Industry University, Azadlig Ave. 20, Baku AZ1010, Azerbaijan
[3]Dept. of Bible, Archaeology, and Ancient Near East, Ben-Gurion University, Be'er-Sheva, Israel

The modern state of Israel is located between 29o and 33o north of the Earth's equator. It is a small (about 22,000 km2) subtropical region between the temperate and tropical zones, characterized chiefly by semi-arid and arid climates. Such climate causes increased productivity and water-use efficiency due to elevated CO2, which tends to increase ground cover, counteracting the effects of higher temperatures. As a result of this effect, Israel, while small, exhibits complex soil formations with variable physical properties, even within small areas. Despite its comparatively diminutive dimensions, Israel has been a focus of human exploitation and settlement since the earliest days of human expansion. More than 27,000 recorded sites form a long record of human presence in the area, starting around 1.5 Mya, presenting one of the densest national archaeological records in the world. While some sites are still clearly visible on the surface, most ancient remains of various ages and origins occur in the subsurface layers at depths of 0.5-8 m (usually in multi-layered archaeological sites). Hundreds, if not thousands, of new sites are discovered yearly due to construction and development activities, and more than 300 salvage excavations are conducted by the Israel Antiquities Authority yearly. Traditional archaeological survey methods are based on covering transects of areas by foot and, while prolific, are by nature highly time-consuming and costly. Moreover, they usually do not supply information on the extent and character of sub-surface remains. Different attempts have been made over the years to apply surface geophysical methods (e.g., GPR, ERT, magnetic, paleomagnetic, subsurface seismics, self-potential, thermal, VLF, induced polarization, piezoelectric, and microgravity) for the identification of archaeological remains as rapid, effective, and noninvasive alternatives for 'traditional' archaeological survey methods. However, these attempts have not always been successful, mainly because of the environmental variability and complex physical-archaeological conditions. Remote Sensing (RS) is a low-expensive tool used for detecting and monitoring the physical attributes of objects of interest on or below the Earth's surface from a considerable distance. RS has been proven instrumental in

archaeological investigations and in comprehending historical contexts on a large scale. This is attributed to RS's rapid data acquisition, expansive coverage, high resolution, and spectral sensitivity to anomalies associated with surface, subsurface, buried, and underwater archaeological features. Archaeologists gain aid in enhanced discoveries and comprehension of archaeological context by utilizing passive and active sensors on drones, satellites, aircraft, and uncrewed aerial vehicles. Active RS (such as radar and LiDAR) offers advantages in detecting buried sites in deserts or concealed archaeological landscapes within forested areas compared to passive RS (encompassing photography and multi-/hyperspectral techniques). The advanced RS application in Israel enabled unmasking unknown archaeological targets in the Wadi Asekt (northern Israel) and the Biq'at Sayyarim (southern Israel). Detailed surface geophysical studies (GPR and magnetic) and archaeological investigations will be conducted at the following stage in the selected areas. Information theory approaches and modern wavelet methodologies will be applied to integrate RS data numerically with geophysical (and possibly geochemical) methods.

Keywords: geophysical tools, information criteria, Bayes estimation, Remote Sensing, machine learning, integrating different methods

I. Introduction

All geophysical (archaeological, geological) studies are applied in definite succession in time and space. Different geophysical and archaeological means (e.g., geophysical mapping and localization, geomorphological studies, geochemical investigations, and excavations) are employed to solve different archaeological (environmental) problems. Apparently, the most effortlessly formalized are digital geophysical observations.

The final expected aim of the geophysical (environmental) analysis is the best investigation of the studied area by *a priori* assumed limitations. The effectiveness of the geophysical tool application is based on three main factors: (1) cost (criterion C), (2) time (Criterion T), and (3) informational (criterionΠ). 1st and 2nd criteria may be estimated by simple calculation but determining the 3rd criterion is a complex problem. The informational criterion model consists of three components (Eppelbaum et al., 2003): (1) quantitative estimation of information, (2) estimation of informational reliability, and (3) estimation of informational value according to the pragmatic criteria (Figure 1). The paper aims to determine a set of tools that compose the notion of "geophysical prospecting" by assuming the reliability of the means. Reliabilities of information obtained by separate tools and sets of tools are analyzed in detail. The suggested procedure for determining the reliability of tools and sets of tools is based on an improved methodology of conditional probability utilization.

Our aim in this investigation is the estimation of criterion Π. All available geophysical/environmental information can be represented in the classic three-level variant: (a) syntactical – volume of information, (b) semantic – substance of information, and (c) pragmatic – value of information.

A principal logical-heuristic model of geophysical-environmental information can be described in the following form:

$$\Pi = Q \cup R \cup V \, , \tag{1}$$

where Q is the quantitative estimation of information, R is the estimation of informational reliability corresponding to the semantic criterion, V is the estimation of informational value by the degree of aim achievement according to the pragmatic criterion, and $\cup$ is the symbol of unification.

This algorithm is based on the fundamental terms of information theory and combined with the structural (hierarchical) approach. This approach enables the construction of each indicator as a comprehensive structure reflecting a set of typical situations. After this, the virtual depth of searching is estimated and calculated using the developed informational approach. Realizing the proposed strategy provides quantitative calculation and effective control of geophysical/environmental studies.

In actual conditions, many random factors disturb the results obtained by geophysical means. One essential problem is the impossibility of obtaining a satisfactory formalized description of factors influencing the results of local determinations. Similar situations are known in the theory of "decision making," where a complete math formalization of the investigated problem is complicated. Our experience (Eppelbaum et al., 2003; Eppelbaum, 2014) suggests that applying expert methods in many situations (logical and math-statistical procedures) will be the most effective.

We will consider the reliability of multi-indicator prospecting at the level of local determination and examine the reliability of information obtained by a separate means or set of means. The main aim of the paper is the problem of determining a set of means composing the notion of "geoinformation prospecting" (relative to some fixed feature) by assumed reliabilities of the means (in contrast to (Eppelbaum, 2014, 2020) where mainly statistical criteria were analyzed). Solving this problem will allow us to find the most optimal combinations of investigation means in different physical-geological conditions.

The determination of the reliability of separate means, broadly speaking, may be obtained by the results of control observations or by expert methods.

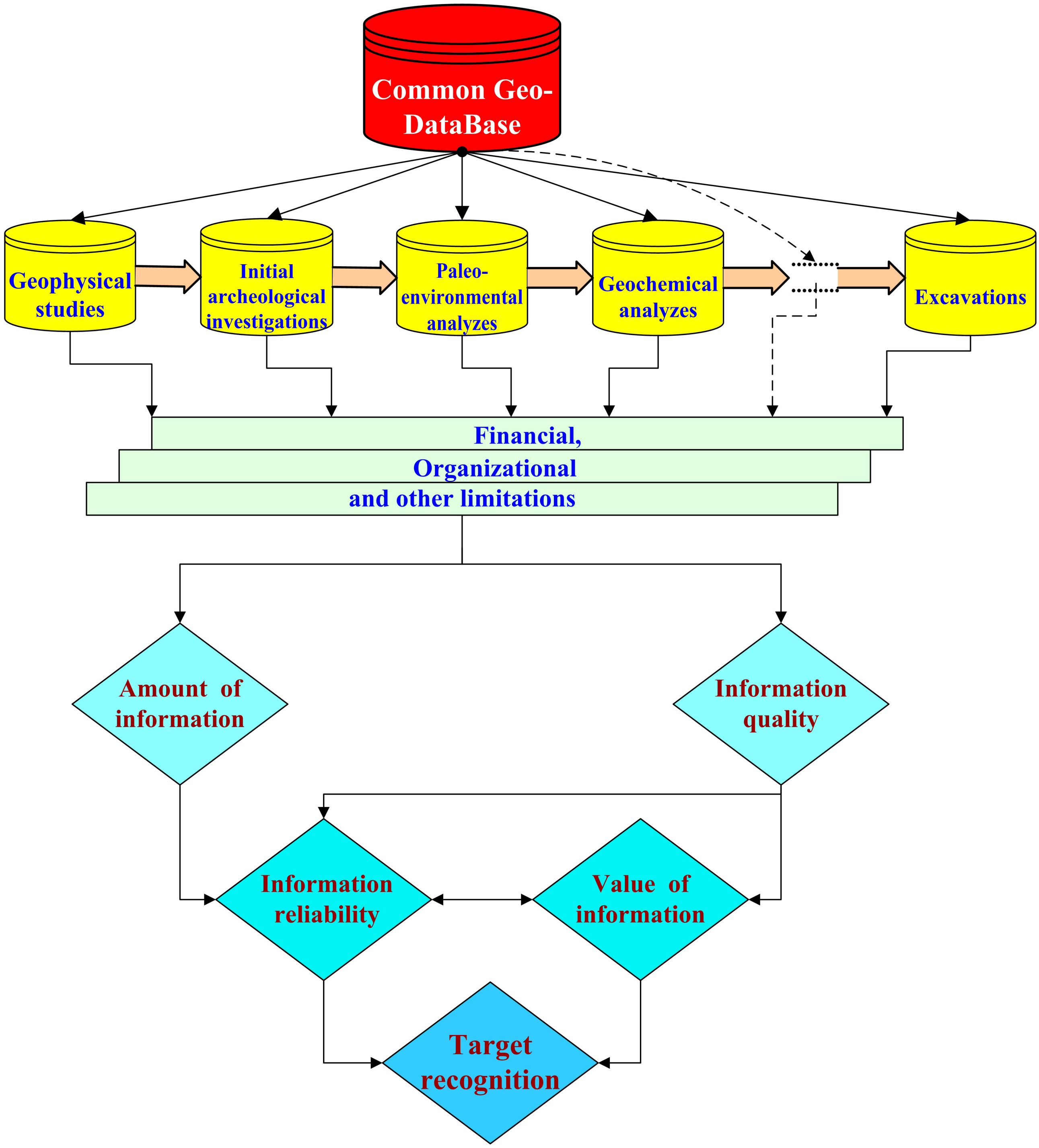

Figure 1. Common scheme of geo-information (modified after Eppelbaum, 2020)

2. Simplified probabilistic estimation of geophysical (environmental) information

Let us study geophysical observations here, as they are more easily quantitatively formalized.

The geophysical fields applied in geology (environment, archaeology) usually have maximal and minimal intensity within studied areas. The difference between the maximal and minimal intensities may be subdivided into some intervals (gradations). Gradations of indicators can also be used to obtain information about the types of anomalous target(s) (**AT**). Physical fields, geochemical analyses, environmental features, etc., can be indicators. Let $P(A_i|B)$ denote the posterior probability of finding the *i*-th gradation of indicator A (e.g., magnetic field intensity) over the targets B, $P(A_i)$ is the prior probability of finding the same gradation in a survey area. Thus, partial information on the presence of the target $I_{A_i \to B}$ contained in the recorded A_i gradation takes the following form:

$$I_{A_i \to B} = \log_2 \left[\frac{P(A_i|B)}{P(A_i)} \right], \tag{2a}$$

as the uncertainty in the recording of A_i before the survey was $\log_2 P(A_i)$ and after the survey – $\log_2 P(A_i|B)$.

Similarly,

$$I_{A_i \to \overline{B}} = \log_2 \left[\frac{P(A_i|\overline{B})}{P(A_i)} \right]. \tag{2b}$$

Statistically, the probabilities (or, more precisely, relative frequencies) are expressed by the following ratios: S is the total number of values, S_i is the number of values occupied by the *i*-th interval of the A_i values, S_p is the total number of points reflecting the **AT** projections to the earth's surface, and S_{pi} is the number of points common for the interval A_i and the **AT** projections.

Then:

$$P(A_i) = \frac{S_i}{S}, \quad P(A_i|B) = \frac{S_{pi}}{S_p}, \quad P(A_i|\overline{B}) = \frac{S_i - S_{pi}}{S - S_p}. \tag{3}$$

The increment in information contained about the presence of the object

$$\Delta I_i = I_{A_i \to B} - I_{A_i \to \overline{B}} = \log_2 \left[\frac{P(A_i|B)}{P(A_i|\overline{B})} \right]. \tag{4}$$

each elementary cell of the studied geophysical (archaeological) characteristics are summed up.

3. Information Theory for a Set of Methods: Some Mathematical Background

Let us consider a more complex case when we try to convolute information from different principal geoinformation tools. Let us assume that feature R is any independent characteristic of the archaeological (environmental) target, such as thickness, density, radioactivity, color, weathering, etc.; mean S is some investigation procedure providing information about the direct or circumstantial geological-geophysical feature (features), such as drilling, geophysical prospecting, geological mapping, geochemical analyses, etc.

Beneath the reliability of tool (mean) *S* concerning feature *R,* we will comprehend a probability of certainty for hypothesis Γ: the value of feature *R* equals the value obtained by mean *S*. Symbol $S = \{S_i\}_{i=\overline{1,n}}$ will designate an arbitrary integration of various means (geophysical, archaeological, geological, etc.).

If features' values are measured on a numerical scale, we will consider this feature quantitative; otherwise, we will believe that the feature is qualitative. The main difference between quantitative and qualitative means is that numerical scales of quantitative features are ordered, while in a typical case, the scale of qualitative parameters has no order.

Let us *S* and *R* are the fixed mean and feature, respectively, and $\{r_1, r_2, \ldots, r_k\}$ are set of values, which may include feature *R*. We will consider that the result of the local determination of feature *R* by mean *S* always consists of some alternative r_τ, $1 \le r \le k$, which may differ from the actual value of feature *R*.

If the continuous scale of feature *R* has been divided into intervals, then the determination of R reduces to finding the concrete interval to which this feature is. In this case, we can consider that r_1, r_2,…, r_k are the points belonging to intervals of dividing (for instance, middles of these intervals). Obviously, among the values r_1, r_2,…, r_k is always such r_t, which belongs to the same interval as the real value of feature *R*. Then the difference between the actual value of feature and value r_t does not exceed the length of the respective interval, and value r_t may be considered as real since we propose that dividing of scale for feature *R* is being with the necessary accuracy (Eppelbaum et al., 2023). Further, under the real value of feature *R*, we will imply the mentioned value r_t.

3.1. Problem Statement

The introduced notion of reliability of mean *S* relative to feature *R* is a quantitative measure of the frequency of feature R (obtained by using mean *S*) coinciding with its actual value. A case when feature *R* is determined not by one mean *S*, but by a set of means $S = \{S_i\}_{i=\overline{1,n}}$ has the following peculiarity. Any series of observations (analyses) realized by a set *S* is defined, obviously, not one alternative r_τ, but a set of alternatives $r_{\tau_1}, r_{\tau_2}, \ldots, r_{\tau_n}$, that are different ones. In this case, we cannot talk about one value of feature R generated by a set S. Then the following question arises having a set of obtained values R - $\left(r_{\tau_1}, r_{\tau_2}, \ldots, r_{\tau_n}\right)$, which alternative r_τ needs to be recognized as the value of feature R. In other words, which *a priori* hypotheses from set k (the actual value of R equals to r_t, $1 \le t \le k$) may be assumed as the most suitable. The selection of the best hypothesis should be realized using some algorithm (rule). Formally, such a rule may be considered as a mapping $\aleph$ of a set of possible indications of means $\left(r_{\tau_1}, r_{\tau_2}, \ldots, r_{\tau n}\right)$ to the set of values of features $\{r_t\}_{t=\overline{1,k}}$:

$$\aleph : \left\{\left(r_{\tau_1}, r_{\tau_2}, \ldots, r_{\tau_n}\right)\right\}_{(\tau_1, \tau_2, \ldots, \tau_n)} \to \{r_t\}_{t=\overline{1,k}} . \tag{5}$$

If we will associate some fixed rule $\aleph = \aleph(S, R)$ with each feature R and set of means $S = \{S_i\}_{i=\overline{1,n}}$, then we will consider that S uniquely determines R. Really, a series of local observations of feature R defines a set of alternatives $r_{\tau_1}, r_{\tau_2}, \ldots, r_{\tau n}$, and the rule $\aleph$ gives to the set one single value $\aleph\left(r_{\tau_1}, r_{\tau_2}, \ldots, r_{\tau n}\right)$ of the feature R.

However, finding the formalizability of reliability is a complex mathematical problem, and there are no ways (at least comparatively simple ways) for an identical definition of the rule $\aleph$. In a typical case, if $\aleph_1$ and $\aleph_2$ are two different rules, their comparison is a complex problem (Eppelbaum, 2020).

The proposed probabilistic approach to defining reliability enables forming some criterion for comparing rules and solving simultaneously a problem of selection (criterion) rule. Let us suppose that the value of feature R is r_1 for definiteness. Results of determination R by mean S may differ from r_1 because of the determination inaccuracy. A set of possible indications of mean S may be described using some probability distribution:

$$P_{11} = P\left(r_1^o \middle| r_1^r\right),\ P_{12} = P\left(r_2^o \middle| r_1^r\right), \ldots,\ P_{1k} = P\left(r_k^o \middle| r_1^r\right), \tag{6}$$

where $P_{1\tau} = P\left(r_\tau^o \middle| r_1^r\right)$ is the conditional probability of that results of determination is r_τ if the real value of feature R is r_1 (indexes “o” and “r” designate the “observed” and “real” values, respectively).

Value r_2 of feature R corresponds to another set of probabilities: P_{21}, P_{22}, …, P_{2k}. In the typical case, probabilities P_{t1}, P_{t2}, …, P_{tk} depend on t (i.e., the actual value of feature R). We will consider a matrix of conditional probabilities $\left\{P_{tr} = P\left(r_\tau^o \middle| r_t^r\right)\right\}_{t,\tau=\overline{1,k}}$ for each pair (S, R) by introducing expert methods since obtaining it logically is practically impossible:

$$\Re(S,R)=\begin{pmatrix} P_{11} & \dots & P_{1k} \\ \dots & \dots & \dots \\ P_{k1} & \dots & P_{kk} \end{pmatrix}. \tag{7}$$

We must note that the matrix depends not only on S and R but also on the concrete physical-geological (environmental, archaeological, etc.) factors. However, the relationship of $\Re$ (S, R) from different factors is not discussed here since we believe these factors are fixed in natural conditions.

Obtaining a matrix (S, R) containing k_2 numbers may appear to be a practically unsolvable problem. However, in natural conditions, the number of independent elements in this matrix is usually significantly reduced.

It was mentioned above that probabilities $P_{t\tau}$ are conditional ones. $P_{tr} = P\left(r_\tau^o \middle| r_t^r\right)$ is the conditional probability of observed value r_τ of feature) indicator) R (under the condition that r_τ is the actual value of the feature). However, an inverse problem may be of vital importance (Eppelbaum, 2020): when using the observed indication of mean, it's necessary to give a probabilistic estimation of real value. Mathematically, this offers solutions to the problem of determining probabilities $\left\{\tilde{P}_{\tau t} = P\left(r_\tau^r \middle| r_t^o\right)\right\}_{t,\tau=\overline{1,k}}$. In contradiction to $P_{t\tau}$, indexes "o" and "r" here are interchanged.

Probabilities $\tilde{P}_{\tau t}$ are not associated with $P_{t\tau}$ a challenging analytical relationship. However, if *a priori* probabilities $P(r_t)$ of alternative R values are known, then values $\tilde{P}_{\tau t}$ may be expressed by $P_{t\tau}$ using well-known Bayes's expression (e.g., Daston, 1995):

$$\tilde{P}_{\tau t} = P\left(r_t^r \middle| r_\tau^o\right) = \frac{P\left(r_\tau^o \middle| r_t^r\right)P(r_t)}{\sum_{t=1}^{k} P\left(r_\tau^o \middle| r_t^r\right)P(r_t)} \quad . \tag{8}$$

If we have no initial information about the values of the feature, we will consider that $P(r_1) = P(r_2) = \dots = P(r_k) = 1/k$. In this case, Eq. (8) will be simplified:

$$\tilde{P}_{\tau t} = P\left(r_t^r \middle| r_\tau^o\right) = \frac{P\left(r_\tau^o \middle| r_t^r\right)}{\sum_{t=1}^{k} P\left(r_\tau^o \middle| r_t^r\right)} \quad . \tag{9}$$

Thus, if for all τ is fulfilled, the following equality:

$$\sum_{t=1}^{k} P\left(r_\tau^o \middle| r_t^r\right) = 1, \tag{10}$$

then $P\left(r_\tau^o \middle| r_t^r\right) = P\left(r_t^r \middle| r_\tau^o\right)$. Equality (10) indicates that a sum of elements of any column of the matrix $\Re\ (S, R) = 1$.

Further, we will suppose that $P(r_1) = P(r_2) = ... = P(r_k) = {}^1\!/_k$, i.e. alternatives r_1, r_2, …, r_k have *a priori* the equal probabilities. At the same time, fulfilling equality (10) is not obligatory.

3.2. Reliability of mean S relative to feature R

From the above-mentioned description of the total probability (Daston, 1995), it follows that the reliability of mean S relative to feature R may be calculated using the following expression

$$d(S;R) = \sum_{\tau=1}^{k} P\left(r_\tau^o\right) \cdot P\left(r_\tau^r \middle| r_t^o\right). \tag{11}$$

Considering that

$$P\left(r_\tau^o\right) = \sum_{\tau=1}^{k} P\left(r_t^r\right) P\left(r_\tau^o \middle| r_t^r\right) = \frac{1}{k} \sum_{t=1}^{k} P\left(r_\tau^o \middle| r_t^r\right)$$

and

$$P\left(r_\tau^r \middle| r_\tau^o\right) = \frac{P\left(r_\tau^o \middle| r_\tau^r\right)}{\sum_{t=1}^{k} P\left(r_\tau^o \middle| r_t^r\right)} ,$$

Eq. (11) has been transformed to the following form:

$$d\left\{\begin{aligned} &(S;R) = \sum_{\tau=1}^{k}\left(\frac{1}{k}\sum_{t=1}^{k} P\left(r_\tau^o \middle| r_t^r\right) \frac{P\left(r_\tau^o \middle| r_\tau^r\right)}{\sum_{t=1}^{k} P\left(r_\tau^o \middle| r_t^r\right)}\right) \\ &= \frac{1}{k}\sum_{\tau=1}^{k} P\left(r_\tau^o \middle| r_\tau^r\right) = \frac{1}{k}\sum_{\tau=1}^{k} P_{\tau\tau} \ . \end{aligned}\right\}. \tag{12}$$

3.3. Reliability of set of means S_i relative to feature R

Let us consider the definition of feature R by a set of means $S = \{S_i\}_{i=\overline{1,n}}$. The proposed methodology is based on realizing the following proposition.

Let us assume that the sequence of indications of means $S = \{S_i\}_{i=\overline{1,n}}$ (replacing feature R) is an independent one. This means that

$$P\left(r_{\tau_1}^o, r_{\tau_2}^o, ..., r_{\tau_n}^o \middle| r_t^r\right) = P\left(r_{\tau_1}^o \middle| r_t^r\right) \cdot P\left(r_{\tau_2}^o \middle| r_t^r\right) \cdot ... \cdot P\left(r_{\tau_n}^o \middle| r_t^r\right). \tag{13}$$

As aforementioned, we need to agree on which *R* value we will select as the most plausible hypothesis about its real value (by each fixed set of indications of means).

After series of observations of feature *R* (using a set of means $S = \{S_i\}_{i=\overline{1,n}}$), we will receive a set of alternatives $r^o_{\tau_1}, r^o_{\tau_2}, ..., r^o_{\tau_n}$. Which of the following *k* hypotheses Γ_t ($r^r_t = r^0_t$) could be adopted as the most plausible? There must exist a hypothesis for which the respective probability

$$P\left(r^r_t \middle| r^o_{\tau 1}, r^o_{\tau 2} ..., r^o_{\tau n}\right) \tag{14}$$

will admit the maximum value.

We designate that ℵ* is mapping (rule) placing in requirement to each sequence of means such alternative value r_t* of feature *R*, on which is reaching the maximal value of Eq. (14). We will propose that the reliability of a set of means *S* relative to feature *R* is the probability of coinciding feature *R* (determined by the rule ℵ*) with the actual *R* value (Eppelbaum et al., 2003).

Taking into this proposition and the known expression of the total probability, we have

$$d(S_1, S_2, ..., S_n; R) = \sum\nolimits_{(\tau_1, \tau_2, ..., \tau_n)} P\left(r^o_{\tau_1}, r^o_{\tau_2}, ..., r^o_{\tau_n}\right) \cdot P\left(r^r_{t*} \middle| r^o_{\tau_1}, ..., r^o_{\tau_n}\right). \tag{15}$$

Transforming (15) analogously to the conversion of Eq. (11) to Eq. (12), we receive the following expression for the calculation of the reliability of set *S* relative to feature *R*:

$$d(s_1, s_2, ..., s_n; R) = \frac{1}{k} \sum\nolimits_{(\tau_1, \tau_2, ..., \tau_n)} P_{t*\tau_1} \cdot P_{t*\tau_2} \cdot ... \cdot P_{t*\tau_n} . \tag{16}$$

The rule ℵ* setting up a correspondence between the set of possible indications of means $\left\{r^o_{\tau_1}, r^o_{\tau_2}, ..., r^o_{\tau_n}\right\}$ and set of values of feature $\{r_t\}$, sets up a simultaneous correspondence between the indexes:

$$\aleph^* : (\tau_1, \tau_2, ..., \tau_n) \rightarrow t^* . \tag{17}$$

It is supposed that *t** in Eq. (16) is defined from a relationship (17) for each fixed set $(\tau_1, \tau_2, ..., \tau_n)$.

4. Remote Sensing Image Recognition

4.1. Some Common Background

Remote Sensing (RS) encompasses all methods used for detecting and monitoring the physical attributes of objects of interest on or below the Earth's surface from considerable distances (Lasapo nara and Masini, 2012; Luo et al., 2018, 2023; Colombero et al., 2020). RS has been proven instrumental in archaeological investigations and in comprehending historical contexts on a large scale (e.g., Chen et al., 2017; Fiorucci et al., 2022; Price et al., 2023; Tiwari et al., 2023). This is attributed to RS's rapid data acquisition, expansive coverage, high resolution, and spectral sensitivity to anomalies associated with surface, subsurface, buried, and underwater archaeological features. Significant discoveries were made using RS applied to archaeological landscapes, encompassing paleo-environments, ancient settlements, communities, and anthropogenic surroundings (Yang et al., 2022). Utilizing passive and active sensors on drones, satellites, aircraft, and unmanned aerial vehicles, archaeologists gain a spatial viewpoint that aids in enhanced discoveries and comprehension of archaeological (Birkenfeld and Garfunkel, 2020) context.

Active RS (such as radar and LiDAR) offers advantages in detecting buried sites in deserts or concealed archaeological landscapes within forested areas compared to passive RS (encompassing photography and multi-/hyperspectral techniques). Archaeological RS can be combined with ground-based geophysical methods (e.g., ground-penetrating radar (GPR), electrical resistivity tomography (ERT), magnetics, electromagnetic sensing, and acoustic sensing (e.g., multibeam bathymetry and sonar). These geophysical and acoustic methods can complement satellite and aerial RS findings. Ground-based geophysical methods like GPR, magnetometry, or ERT can then be applied to explore and confirm the presence of subsurface features identified through satellite remote sensing. For instance, anomalies detected in satellite imagery indicating potential buried structures or features can be confirmed and mapped using GPR or electrical resistivity surveys on the ground (e.g., Deroin et al., 2012). Anomalies in satellite images may correspond to buried settlements or structures, and magnetometry can verify and map these features. This integration enhances the understanding and recording of buried structures or cultural landscapes.

Machine learning techniques can be used to make integrated studies more effective. Machine learning (or computer vision methods) has significantly transformed remote sensing data analysis by enabling advanced algorithms to process vast quantities of imagery from satellites and aerial platforms (Davis, 2019). Recent advancements in semi-supervised and unsupervised machine learning techniques extend the exploration of extensive datasets. Convolutional neural networks (CNNs) excel in extracting intricate spatial features and facilitating land cover classification, semantic segmentation, change detection, and super-resolution imaging (Meyer-Heß et al., 2022). Machine learning algorithms enable anomaly detection and enhance understanding of patterns typical for archeological sites.

Pre-processed images can be used to train neural networks and develop models of automatic recognition of archeological objects. Several models must be created for this aim since each neural network is trained on a particular class of objects (round-shaped, square-shaped, elongated), sometimes allowing us (combined with additional factors) to recognize a specific epoch. Machine learning for this aim encompasses supervised and unsupervised learning methods, including clustering, regression, and classification. Deep learning, a subset of machine learning, employs complex algorithms like CNNs for object detection and image analysis tasks. Unlike traditional methods, artificial intelligence-based models can handle large datasets without predefined rules, making them valuable for tasks requiring new data predictions. The choice between these approaches depends on the specific application and research goals. In our study, we will train neural networks to recognize archeological objects of different shapes and epochs.

Three image processing algorithms most popular in computer vision will be tested, namely, Single Shot Detection (SSD), Faster Region-based Convolutional Neural Networks (Faster R-CNN), and YOLO - You Only Look Once (Srivastava et al., 2021). SSD employs a single neural network to predict object bounds and class probabilities concurrently. It applies convolutional layers to the input image and predicts multiple bounding boxes and their associated class probabilities across different spatial scales. R-CNN is faster and operates in two stages. First, it employs a region proposal network to propose potential bounding box regions, and then a network head processes these regions for object classification and bounding box refinement. YOLO employs a single-stage approach technique, directly predicting bounding boxes and class probabilities on a grid system overlaid on the image. YOLO divides the image into a grid and predicts bounding boxes and their corresponding class probabilities within each grid cell. This approach enables faster processing since it eliminates the need for regional proposals. SSD and YOLO are considered single-shot detectors due to their ability to predict objects in one pass, and Faster R-CNN uses a two-stage process involving region proposals and classification. As a result, Faster R-CNN tends to have greater accuracy but is relatively slower compared to SSD and YOLO. SSD and YOLO prioritize speed, achieving a balance between speed and accuracy. YOLO optimizes speed by directly addressing object detection and classification in one step. Faster R-CNN, although slower, often delivers higher precision due to its multi-stage approach, allowing for more precise localization and classification of objects.

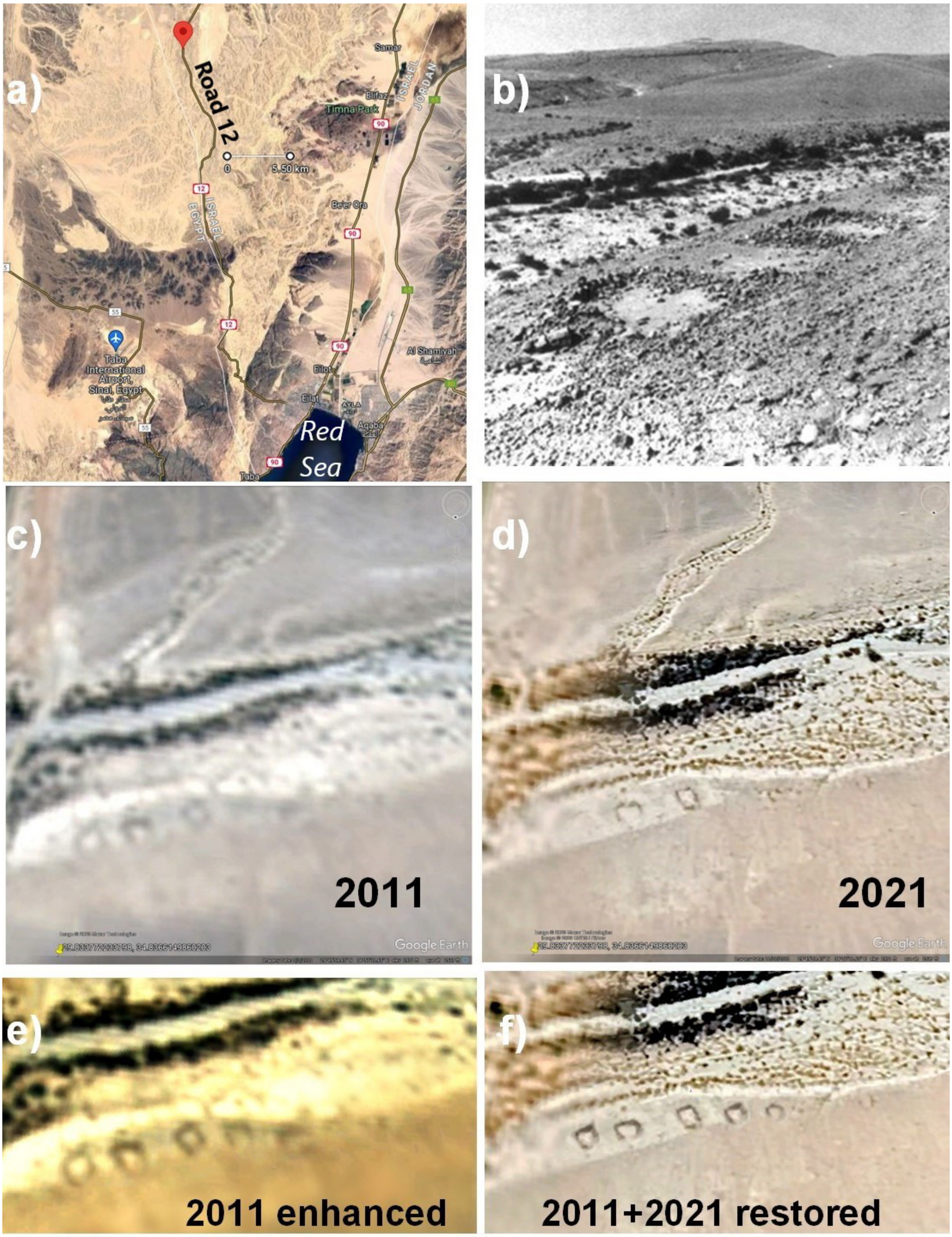

Figure 2. Restoration of the image of the Biq'at Sayyarim site (southmost Israel). (a) general location, (b) on-site photo, (c) satellite image taken in 2011, (d) satellite image taken in 2021, (e) enhanced image of the site based on 2011, (f) restored image from the combined 2011 and 2021 images (Eppelbaum et al., 2024a, 2024b).

Choosing the best method for our task requires considering the balance between accuracy, speed, and computational resources in the context of the specific requirements of archaeological site identification. Conducting comparative studies or trials with the available methods on the target dataset will help us determine which approach best suits the given application. When archaeological site identification requires precise localization and classification of small or intricate details within the satellite imagery, Faster R-CNN might be more suitable due to its multi-stage approach. However, preliminary studies show that SSD and YOLO can excel in finding larger-scale objects. The process will include (i) collecting a labeled dataset and preprocessing the data, splitting it for training, validation, and testing, (ii) choosing a suitable CNN architecture, (iii) augmenting the data to improve model robustness, (iv) training the CNN with appropriate hyperparameters and regularization, (v) evaluating the model's performance on the validation dataset, (vi) fine-tuning and testing on a separate dataset, (vii) deploying the model for archaeological object recognition, and (viii) updating and refining the model as new archaeological objects are discovered or as the recognition requirements evolve. In the next stage, we will analyze pre-processed images of an area of interest taken in different seasons and in a different light, which practically allows the restoration of a 3D picture of the objects.

Geophysical surface studies (in our case – precise magnetic investigations) will confirm the archaeological recovery results obtained at the previous stage. We will apply informational procedures for numerical integration of the data derived from the independent physical data. For this aim, the remote sensing and magnetic field data will be converted to specific informational units, and their algebraic sums will be calculated. Based on the *a priori* assumed thresholds, the anomalous zones corresponding to buried archaeological remains will be recognized.

4.2 Example of a machine learning technique applied to remote sensing in northern Israel: Detecting earlier unknown targets

The Early or Middle Bronze Age object is located about 1 km north of Ramathania (Figure 3), on the north bank of Nahal Zytan (northern Israel). It was reported as a site consisting of two concentric circles built of medium-sized field stones. The outer circle's diameter is ~73 m, and the inner circle is ~ 30 m wide. Figure 4a shows the on-site photo of the object, and Figure 3b is the aerial photo of the set of two circles.

It is well known that an onsite survey often does not allow recognition of regular patterns in large-scale archeological objects with typical sizes larger than tens meters, first, because of their typical poor condition and a wide scattering of the building material and, second, because of specificity of brain processing of the images incomparable with human size. In the case of the object shown in Figure 4, the aerial image gives a better understanding of its shape and peculiarities.

Meanwhile, sometimes remote sensing images can provide even more information. Figure 4c is a 2017 image of the site. One can recognize two sets of circles, indicated by numbers 1 and 2, instead of one (shown in Figure 4b). The Israel Antiquities Authority previously identified object 1. The second round-shaped object (2, on the left) (Figure 4c) is far less preserved but still recognizable by the eye. Finally, Figure 4d presents the restored and enhanced image shown in Figure 4c.

Figure 3. Areal map of the Wadi Asekt (northern Israel) (Eppelbaum et al., 2024a, 2024b).

Using convolution, residual, and generative countermeasure neural networks for image improvement is a global trend not only in photography but also in different scientific disciplines when it is required to solve the so-called image super-resolution problem, restoring, and enhancing blur, noise, poorly exposed and broken images. Various interpolation methods and learning-based upsampling are used. Figure 4d shows a result of the image restoration and enhancement using the TensorFlow Hub Module for Enhanced Super Resolution Generative Adversarial Network. The result is comparable with aerial images. The next step is pattern recognition that can be done with another TensorFlow network https://github.com/tensorflow/models/tree/master/research/object_detection .

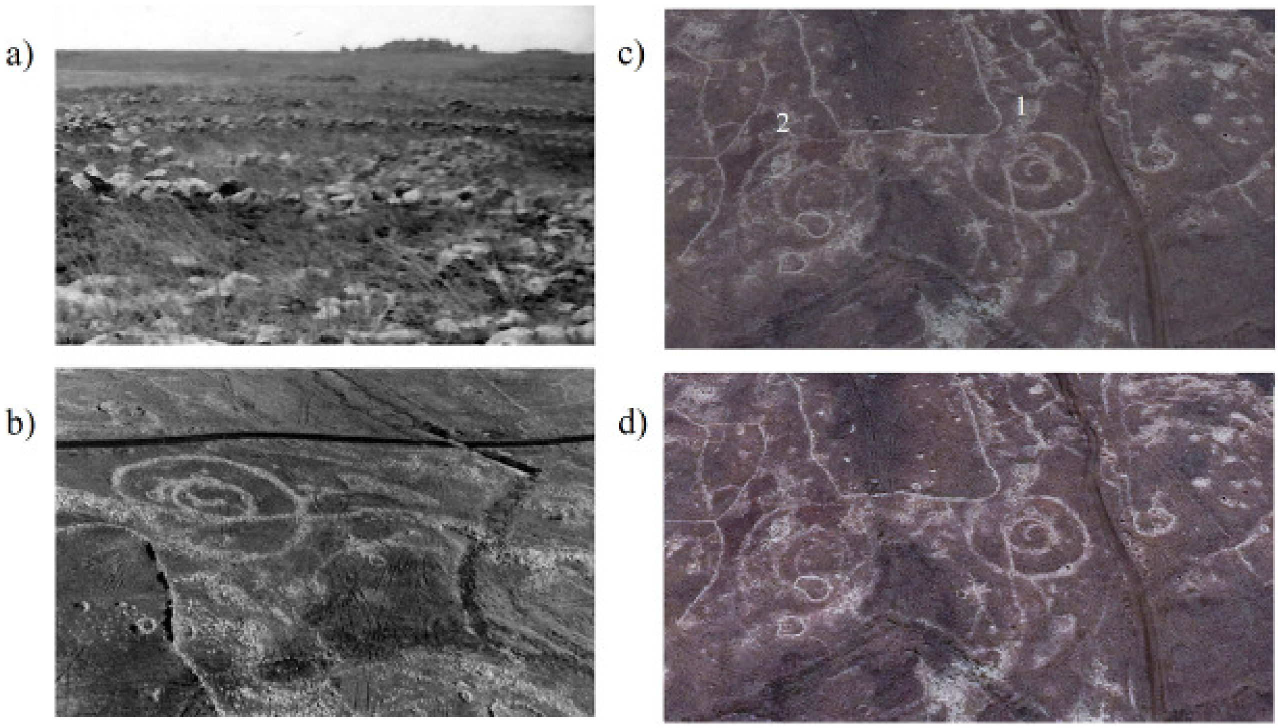

Figure 4. An example of an archaeological object recognizable from space is Object Wadi Asekt, Israel Antiquities Authority map No. 15/1, found by Ben Ephraim Yigal and Hertel Moshe. (a) on-site photo, (b) aerial view to the east, (c) Google Earth Pro 2017 image of the area, (d) Restored and enhanced image (c). Remote sensing image shows two similar round-shaped objects in the area. Circle 1 is object No. 15/1 (Antiquities Authority map), and circle 2 is an unknown object (Eppelbaum et al., 2024a, 2024b).

4.3 Integrating Remote Sensing Data with other geophysical methods

It is most optimal to integrate the RS data with magnetic survey analysis. The developed multicomponent interpreting system includes (e.g., Eppelbaum, 2011, 2015, 2020): (1) removing secondary temporal magnetic variations, (2) a correlation method for eliminating rugged terrain relief, (3) calculation of subsurface layer magnetization, (4) classification of buried magnetized targets on geological and artificial (archaeological), (5) revealing typical archaeological targets by low ratio “signal/noise”, (6) quantitative analysis of magnetic anomalies under oblique magnetization, rugged terrain relief and unknown level of the normal field, (7) 3D magnetic field modeling of complex archaeological-geological sequence, (8) development of Physical-Archaeological Models (PAMs). Remote Operating Vehicle (ROV) survey at various levels over the earth’s surface will provide additional preferences for quantitative analysis of observed magnetic data.

It is also perspective to combine the ROV thermal imaging and Ground Penetration Radar (GPR) surveys in some perspective areas. Thermal imaging based on rock differentiation by thermal properties (Eppelbaum, 2009) will be correlated with the RS patterns. The GPR data (based mainly on the dielectric and electric rock properties (Küçükdemirci, and Sarris, 2022) will be processed using advanced information methodology and correlated with the RS patterns.

Conclusions

1. Application of advanced information-probabilistic methodologies provides an increment of reliability,
2. Employing low-cost remote sensing (RS) methodologies armed with robust modern methodologies allows the discovery of new archaeological remains even in well-studied areas.
3. The advanced application of the RS methodologies in northern and southern Israel allowed the detection of earlier unknown archaeological targets.
4. The RS methodologies may be easily integrated with surface geophysical methods based on presented information-probabilistic technologies.

References

Birkenfeld, M. and Garfinkel, Y. (Eds). 2020. *Digital Archaeology: New research and advanced technologies*. Hebrew University of Jerusalem, Jerusalem (in Hebrew).

Chen, F., You, J., Tang, P., Zhou, W., Masini, N. and Lasaponara, R., 2017. Unique performance of spaceborne SAR remote sensing in cultural heritage applications: Overviews and perspectives. *Archaeological Prospection*, **25**, 71-79. https://doi.org/10.1002/arp.1591

Colombero, C., Comina, C. and Godio, A. (Eds.), 2020. *Remote Sensing in Applied Geophysics*. MDPI, Basel, Switzerland, 309 p.

Daston, L., 1995. *Classical Probability in the Enlightenment*, Princeton University Press, Princeton.

Davis, D., 2019. Object-based image analysis: a review of developments and future directions of automated feature detection in landscape archaeology. *Archaeological Prospection*, **26**, 155–163.

Deroin, J.-P., Téreygeol, F., Cruz, P., Guillot, I. and Méaudre, J.-Ch., 2012. Integrated non-invasive remote-sensing techniques and field survey for the geoarchaeological study of the Sud Lípez mining district, Bolivia. *Jour. of Geophysics and Engineering*, **9**, No. 4, S40–S52.

Eppelbaum, L.V., 2009. Near-surface temperature survey: An independent tool for buried archaeological targets delineation. *Jour. of Cultural Heritage*, **12**, Suppl.1, e93-e103.

Eppelbaum, L.V., 2011. Study of magnetic anomalies over archaeological targets in urban conditions. *Physics and Chemistry of the Earth*, **36**, No. 16, 1318-1330.

Eppelbaum, L.V., 2014. Geophysical observations at archaeological sites: Estimating informational content. *Archaeological Prospection*, **21**, 2, 25-38.

Eppelbaum, L.V., 2015. Quantitative interpretation of magnetic anomalies from thick bed, horizontal plate, and intermediate models under complex physical-geological environments in archaeological prospection. *Archaeological Prospection*, **23**, No. 2, 255-268.

Eppelbaum, L., 2020. Theories of Probability, Information, and Graphs in Applied Geophysics. *In*: (K. Kyamakya, Ed.), *Prime Archives in Applied Mathematics*, Vide Leaf, 1-35.

Eppelbaum, L.V., Birkenfeld, M. and Khabarova, O., 2024a. A Role of Remote Sensing Analysis for Archaeological Purposes in Arid Climate Regions. *Trans. of the 19th EUG Meet.*, Geophysical Research Abstracts, Vol. **26**, EGU24-2892, Vienna, Austria.

Eppelbaum, L.V., Eppelbaum, V.M. and Ben-Avraham, Z., 2003. Formalization and estimation of integrated geological investigations: Informational approach. *Geoinformatics*, **14**, 3, 233-240.

Eppelbaum, L.V., Khabarova, O. and Birkenfeld, M., 2024b. Informational-Probabilistic Technologies and Remote Sensing: A Future of Archaeogeophysics. *Remote Sensing* (submitted).

Eppelbaum, L.V., Khesin, B.E. and Itkis, S.E., 2001. Prompt magnetic investigations of archaeological remains in areas of infrastructure development: Israeli experience. *Archaeological Prospection*, **8**, No. 3, 163-185.

Fiorucci, M., Verschoof-van der Vaart, W.B., Soleni, P., Le Saux, B. and Traviglia, A., 2022. Deep Learning for Archaeological Object Detection on LiDAR: New Evaluation Measures and Insights. *Remote Sensing*, **14**, No. 7, 1694, 1-18.

Khesin, B.E. and Eppelbaum, L.V., 1997. The number of geophysical methods required for target classification: Quantitative estimation. *Geoinformatics*, **8**, 1, 31-39.

Küçükdemirci, M. and Sarris, A., 2022. GPR Data Processing and Interpretation Based on Artificial Intelligence Approaches: Future Perspectives for Archaeological Prospection. *Remote Sensing*, **14**, 3377, 1-11.

Lasaponara, R. and Masini, N., 2012. Remote Sensing in Archaeology: From Visual Data Interpretation to Digital Data Manipulation. In: Lasaponara, R., Masini, N. (Eds.), *Satellite Remote Sensing. Remote Sensing and Digital Image Processing*, Vol. **16**. Springer, 3-16.

Luo, L., Wang, X., Guo, H. et al., 2018. Google Earth as a Powerful Tool for Archaeological and Cultural Heritage Applications: A Review. *Remote Sensing*, **10**(10), 1558, 1-33.

Luo, L., Wang, X., Guo, H., Jia, X. and Fan, A., 2023. Earth observation in archaeology: A brief review. Intern. *Jour. of Applied Earth Observation and Geoinformation*, **116**, 103169, 1-7.

Meyer-Heß, M.F., Pfeffer, I. and Juergens, C., 2022. Application of Convolutional Neural Networks on Digital Terrain Models for Analyzing Spatial Relations in Archaeology. *Remote Sensing,* **14**, 2535, 1-16.

Price, S.J., Adams, M.J. and Tepper, Y., 2023. An integrated spatial approach to archaeological prospection using GIS and pedestrian survey data at Tell Abu Shusha, Israel. *Archaeological Prospection*, **30**, 233-247.

Srivastava, S., Divekar, A.V., Anilkumar, C., Naik, I., Kulkarni, V. and Pattabiraman, V., 2021. Comparative analysis of deep learning image detection algorithms. *Jour. of Big Data*, **8**, 66, 1-27.

Tiwari, A., Silver, M. and Karnieli, A., 2023. A deep learning approach for automatic identification of ancient agricultural water harvesting systems. *Int. Jour of Appl. Earth Observation and Geoinformation*, **118**, 103270, 1-13.

Yang, L., Driscol, J., Sarigai, S., Wu, Q., Chen, H. and Lippitt, C.D., 2022. Google Earth Engine and Artificial Intelligence (AI): A Comprehensive Review. *Remote Sensing*, **14**, 3253, 1-110.